JOURNAL OF VIROLOGY, Apr. 2003, p. 4566–4576 Vol. 77, No. 8
0022-538X/03/$08.00+0 DOI: 10.1128/JVI.77.8.4566–4576.2003

Reovirus σNS Protein Localizes to Inclusions through an Association Requiring the μNS Amino Terminus

Cathy L. Miller,[1] Teresa J. Broering,[1] John S. L. Parker,[1] Michelle M. Arnold,[1,2] and Max L. Nibert[1,2]*

Department of Microbiology and Molecular Genetics[1] and Virology Training Program,[2] Harvard Medical School, Boston, Massachusetts 02115

Received 11 October 2002/Accepted 23 January 2003

Cells infected with mammalian reoviruses contain phase-dense inclusions, called viral factories, in which viral replication and assembly are thought to occur. The major reovirus nonstructural protein μNS forms morphologically similar phase-dense inclusions when expressed in the absence of other viral proteins, suggesting it is a primary determinant of factory formation. In this study we examined the localization of the other major reovirus nonstructural protein, σNS. Although σNS colocalized with μNS in viral factories during infection, it was distributed diffusely throughout the cell when expressed in the absence of μNS. When coexpressed with μNS, σNS was redistributed and colocalized with μNS inclusions, indicating that the two proteins associate in the absence of other viral proteins and suggesting that this association may mediate the localization of σNS to viral factories in infected cells. We have previously shown that μNS residues 1 to 40 or 41 are both necessary and sufficient for μNS association with the viral microtubule-associated protein μ2. In the present study we found that this same region of μNS is required for its association with σNS. We further dissected this region, identifying residues 1 to 13 of μNS as necessary for association with σNS, but not with μ2. Deletion of σNS residues 1 to 11, which we have previously shown to be required for RNA binding by that protein, resulted in diminished association of σNS with μNS. Furthermore, when treated with RNase, a large portion of σNS was released from μNS coimmunoprecipitates, suggesting that RNA contributes to their association. The results of this study provide further evidence that μNS plays a key role in forming the reovirus factories and recruiting other components to them.

The nonfusogenic mammalian orthoreoviruses (reoviruses) are double-stranded (ds) RNA viruses that contain 10 genome segments encased by a multilayered protein capsid (reviewed in reference 26). Following cell entry, plus-sense RNAs representing full-length copies of each of the 10 segments are transcribed and capped by virally encoded enzymes within the infecting particle (primary transcriptase particle) (7, 13, 15, 33). Following extrusion into the cytoplasm (3, 4), these primary transcripts serve both as mRNAs for viral protein translation and as templates for minus-strand synthesis to regenerate the dsRNA genome segments within newly forming particles (1, 31, 34, 41). At least some of these new particles can act as secondary transcriptase particles, producing additional large amounts of the plus-strand transcripts (27, 36, 40). The interactions between viral proteins and RNAs that recruit the necessary components and form the sites of minus-strand synthesis and core assembly have only begun to be elucidated. Furthermore, the involvement of host proteins in these processes has not been well explored.

The replication and assembly of reoviruses occur within distinct structures called viral factories that appear as small phase-dense inclusions throughout the cytoplasm early in infection and become larger and move toward the nucleus as infection proceeds (5, 28, 29). Viral factories are not membrane bound (25) but associate with cytoskeletal elements such as microtubules (11, 12, 28). The viral dsRNA (35), many of the proteins, and partially and fully assembled particles have been localized to the factories (12, 29). However, the assembly and inner workings of the factories are still poorly understood. A viral strain difference in the formation of filamentous versus globular factories has been recently mapped to the reovirus core protein μ2 (28). μ2 from strains that form filamentous factories associates with and stabilizes microtubules, and the association between μ2 and microtubules has been proposed to determine the morphology of the filamentous viral factories by anchoring them to the microtubule network in infected cells (28). A viral strain difference in the rate of inclusion formation has also been mapped to the μ2 protein (25a).

μNS, a major reovirus nonstructural protein, has been recently implicated in viral factory formation (9). μNS is a 721-residue, 80-kDa protein encoded by the M3 genome segment. A second form of μNS, μNSC, thought to lack 40 residues from the amino (N) terminus of μNS, is also detected during infection (38). μNS binds to core particles in vitro, forming large complexes that remain competent for transcription and capping of the viral plus-strand RNAs (8). The bound μNS prevents outer-capsid proteins from recoating the cores, which suggests that during infection μNS may be involved in delaying outer-capsid assembly so that larger amounts of the transcripts can be produced by these particles (8). When expressed in the absence of other viral proteins, μNS forms globular inclusions that are morphologically similar to the globular viral factories seen during infection with certain reovirus strains (9). In addition, μ2 proteins derived from viral strains with either filamentous or globular factories associate with the N-terminal 40

* Corresponding author. Mailing address: Dept. of Microbiology and Molecular Genetics, Harvard Medical School, 200 Longwood Ave., Boston, MA 02115. Phone: (617) 645-3680. Fax: (617) 738-7664. E-mail: mnibert@hms.harvard.edu.

or 41 residues of μNS. When coexpressed with the filamentous form of μ2, μNS colocalizes with μ2 on microtubules in a pattern very similar to that seen during infection (9). These findings have led us to hypothesize that while μ2 plays an important role in anchoring the factories to microtubules, μNS is the primary determinant of factory formation and may be involved in recruiting other components required for RNA assortment, minus-strand synthesis, and core assembly (9).

A second major reovirus nonstructural protein, σNS, has also been implicated in viral factory formation (5, 25a). σNS is a 366-residue, 41-kDa protein encoded by the S3 genome segment. In vitro, σNS binds single-stranded (ss) RNA in a cooperative, sequence-independent manner, with each unit of σNS covering ~25 nucleotides (17, 37). When isolated from reovirus-infected cells, it is found in large (40- to 60S) complexes that dissociate when treated with RNase A (18, 19, 22), suggesting that σNS and RNA form large nucleoprotein complexes during infection. Recombinant σNS expressed in baculovirus-infected cells is found in similar large nucleoprotein complexes, which dissociate into 7- to 9S complexes upon treatment with RNase A or high-salt washes, suggesting that σNS forms small oligomers in the absence of RNA (16). σNS and μNS, as well as the structural protein σ3, have been isolated from infected cells in complexes with viral ssRNA, leading to the proposal that these proteins are involved in preparing the viral transcripts for minus-strand synthesis and packaging into progeny cores (2). σNS has been recently proposed to nucleate viral factories, based on evidence that it localizes to factories throughout infection and that a viral mutant with a temperature-sensitive σNS protein (*ts*E320) is defective for factory formation at restrictive temperatures (5).

To address our hypothesis that μNS may be involved in recruiting other components to reovirus factories, we examined σNS localization when expressed with μNS in the absence of other viral proteins. We found a strong association between σNS and μNS and identified that the N-terminal 40 residues of μNS, which our laboratory has previously shown to be necessary for association with μ2 (9), are also necessary for the association with σNS. This supports our hypothesis that μNSC, which is thought to lack this N-terminal region, plays some role(s) distinct from those of μNS during infection. We further dissected this region, identifying residues 1 to 13 of μNS as necessary for association with σNS, but not with μ2. Deletion of σNS residues 1 to 11, which our laboratory has previously shown to be required for RNA binding by that protein (16), resulted in diminished association of σNS with μNS. Furthermore, when treated with RNase, a large portion of σNS was released from μNS coimmunoprecipitates, suggesting that RNA contributes to their association. The results of this study provide further strong evidence that μNS plays a key role in forming the reovirus factories and recruiting other components to them.

MATERIALS AND METHODS

Cells and viruses. CV-1 cells were maintained in Dulbecco's modified Eagle's medium (DMEM) (Invitrogen Life Technologies, Carlsbad, Calif.) containing 10% fetal bovine serum (HyClone Laboratories, Logan, Utah) and 10 μg of gentamicin (Invitrogen)/ml. Reovirus strains T1L and $T3D^N$ were our laboratory stocks. The designation $T3D^N$ differentiates our laboratory strain from another T3D laboratory strain ($T3D^C$) that has a filamentous viral factory phenotype.

Antibodies and other reagents. Mouse monoclonal antibody (MAb) 3E10 specific for σNS (5) was a generous gift from T. S. Dermody and colleagues (Vanderbilt University, Nashville, Tenn.). Rabbit polyclonal antisera specific for μNS (8), μ2 (9), and σNS (16) have been described previously. In some experiments, Texas Red conjugates of polyclonal antibodies purified from the μNS antiserum were used (preparation described previously [28]). The following secondary antibodies were used as appropriate for different experiments: Alexa 488- or Alexa 594-conjugated goat anti-mouse or anti-rabbit immunoglobulin G (IgG) (Molecular Probes, Eugene, Oreg.), horseradish peroxidase (HRP)-conjugated donkey anti-mouse or anti-rabbit IgG (Pierce, Rockford, Ill.), and alkaline phosphatase-coupled goat anti-mouse or anti-rabbit IgG (Bio-Rad Laboratories, Hercules, Calif.). For microscopy, antibodies were titrated to optimize signal-to-noise ratios. All restriction enzymes were obtained from New England Biolabs (Beverly, Mass.).

Plasmid constructs. All reovirus genes examined in this study were cloned into pCI-neo (Promega, Madison, Wis.). pCI-M1(T1L) (28), pCI-M1($T3D^N$) (28), pCI-M3(T1L) (9), and pCI-M3(41-721) (9) were previously described. The T1L S3 gene was excised from pGEM-4Z:LS3 (16) with *Hin*dIII and *Eco*RI. The *Hin*dIII end was converted to a blunt end using the Klenow fragment. The T1L S3 gene was then ligated to pCI-neo that had been cut with *Nhe*I and *Eco*RI and had its *Nhe*I end converted to a blunt end. This procedure generated pCI-S3(T1L). The T3D S3 gene was amplified by reverse transcription-PCR from reovirus transcripts made from T3D cores (20) by using a forward primer with an *Xba*I site (5′-GGTCTAGATGATTAGGCGTCACCC-3′) and a reverse primer containing an *Eco*RI site (5′-GGGAATTCGCTAAAGTCACGCCTTGTCGT CG-3′). The PCR product and pCI-neo were each digested with *Xba*I and *Eco*RI and then ligated to generate pCI-S3(T3D). To obtain the S3 gene of temperature-sensitive mutant *ts*E320 (14), overlap-PCR mutagenesis was performed (21). A forward mutagenic primer (5′-GTGTTAAATTGCACGCAGTTTAAA CTTGAG-3′) and reverse mutagenic primer (5′-CTCAAGTTTAAACTGCGT GCAATTTAACAC-3′) and the above forward and reverse primers were used to PCR amplify an S3 gene fragment encoding a threonine at amino acid 260 (39). The purified fragment and pCI-S3(T3D) were digested with *Xba*I and *Eco*RI, gel purified, and ligated to generate pCI-S3(M260T). To express the T1L σNS protein lacking amino acids 1 to 11, the mutated T1L S3 gene was removed from the previously constructed pGEM-4Z.LS3.*Xho*I.Δ31-60 (16) with *Xho*I and *Kpn*I. The mutated T1L S3 gene was ligated to pCI-neo cut with *Xho*I and *Kpn*I. This procedure generated pCI-S3(12-366). The portion of the T1L M3 genome segment encoding μNS amino acids 14 to 721 was amplified by PCR with a forward primer containing an *Nhe*I site and a methionine codon (5′-GACTGCTAGCA TGGTTTCCAAGGCCAAACGTGATATATCATCTCTGCC-3′) and a reverse primer (5′-GGCATATAGGTCATCAGGCACAGAGCG-3′) containing a *Blp*I site. The purified product was cut with *Nhe*I and *Blp*I and ligated to pCI-M3(T1L) that had been cut with *Nhe*I and *Blp*I to generate pCI-M3(14-721). The ATG codon introduced at nucleotides 55 to 57 (amino acid 13) in the M3 gene allowed expression of μNS amino acids 14 to 721. The sequences of all portions of plasmids amplified by PCR were determined to ensure they matched those published.

Transfections and infections. For immunostaining experiments, 1.5×10^5 CV-1 cells were seeded the day before infection or transfection in six-well plates (9.6 cm^2 per well) containing 18-mm round glass coverslips. A total of 2 μg of DNA was transfected into cells using 7 μl of Lipofectamine (Invitrogen) in Optimem (Invitrogen) and incubated for 4 h as suggested by the manufacturer. After incubation, fresh DMEM was added to the cells, and they were incubated at 37°C for a further 14 h before processing for immunofluorescence (IF) microscopy. For immunoprecipitation (IP) studies, 3×10^5 cells were seeded onto 60-mm dishes the day before transfection or infection. Two micrograms of DNA was transfected into cells by using 9 μl of Lipofectamine in Optimem and incubating for 4 h at 37°C. After incubation, fresh DMEM was added to the cells, and they were incubated for a further 14 h at 37°C before preparing for IP. For both immunostaining and IP experiments, cells in dishes or on coverslips were inoculated with T1L or $T3D^N$ reovirus at a multiplicity of 10 PFU per cell in phosphate-buffered saline (PBS; 137 mM NaCl, 3 mM KCl, 8 mM Na_2HPO_4 [pH 7.5]) supplemented with 2 mM $MgCl_2$. The virus was adsorbed for 1 h at room temperature, at which point fresh medium was added. Infected cells were then incubated at 37°C for an additional 5 to 19 h before processing for IF microscopy or IP.

Immunostaining and IF microscopy. Infected or transfected cells were fixed by incubation at room temperature with 2% paraformaldehyde in PBS for 10 min, followed by 3 min at −20°C in 100% ice-cold methanol. Fixed cells were washed three times in PBS and permeabilized for 5 min in 0.2% Triton X-100 in PBS. Cells were again washed three times in PBS and blocked for 5 min in 0.1 M glycine in PBS. Primary and secondary antibodies were diluted in 0.1 M glycine

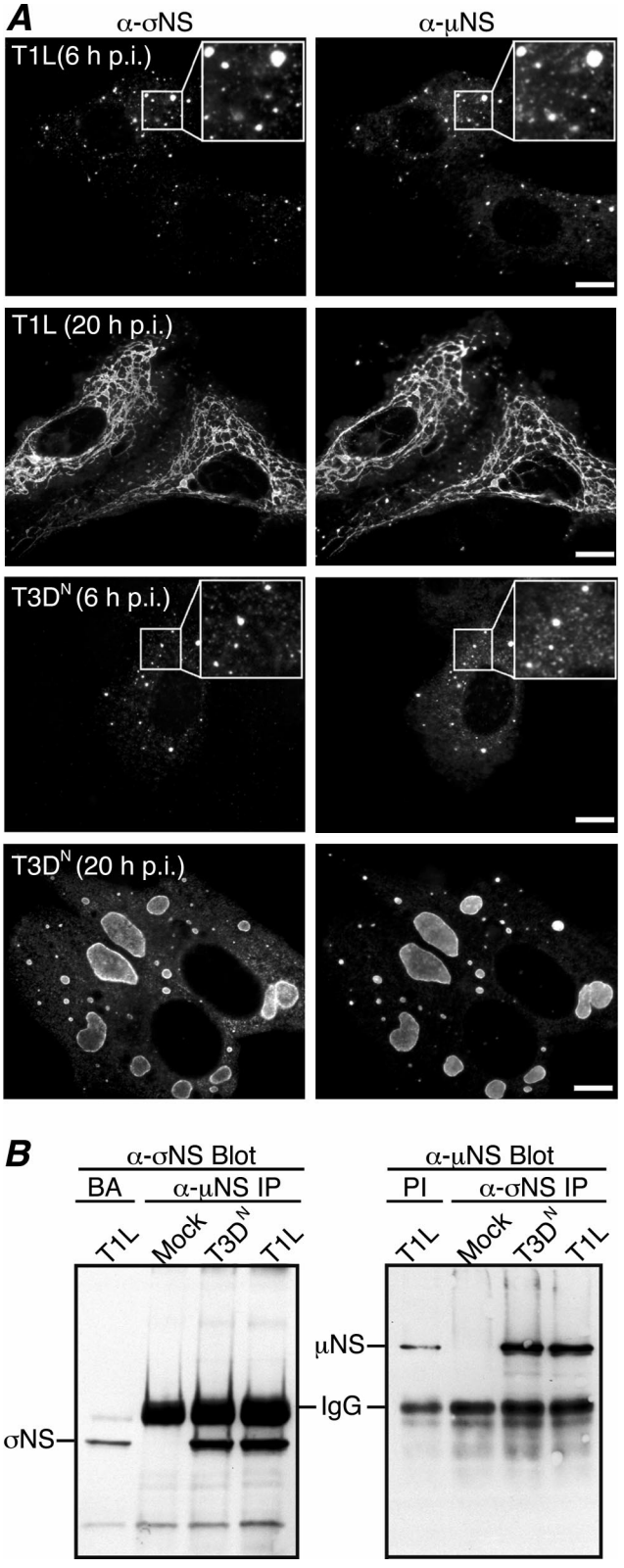

FIG. 1. Colocalization and co-IP of σNS and μNS in T1L- and T3D^N-infected CV-1 cells. (A) IF microscopy of CV-1 cells infected with reovirus T1L (top two rows) or T3D^N (bottom two rows) at 6 h p.i. (first and third rows) or 20 h p.i. (second and fourth rows). The subcellular localizations of σNS and μNS were, respectively, detected by immunostaining with σNS-specific mouse MAb 3E10 (5) followed by Alexa 488-conjugated anti-mouse IgG (left column) and Texas Red-conjugated μNS-specific polyclonal antibodies (9) (right column). Insets show higher-magnification views of the σNS and μNS staining patterns at 6 h p.i. Scale bars, 10 μm. (B) Co-IP of σNS and μNS from T1L- and T3D^N-infected CV-1 cells. At 18 h p.i., T1L-, T3D^N-, or mock-infected CV-1 cells were lysed in nondenaturing buffer and immunoprecipitated (IP) with μNS-specific rabbit polyclonal antiserum (8) (left) or σNS MAb (right). Protein A-Sepharose beads alone (BA) or with rabbit preimmune serum (PI) were used as controls. Immunoprecipitated proteins were separated by SDS-PAGE, transferred to nitrocellulose, and immunoblotted with σNS-specific rabbit polyclonal antiserum (16) followed by HRP-conjugated anti-rabbit IgG (left) or with μNS antiserum followed by HRP-conjugated anti-rabbit IgG (right). Bound HRP conjugates were detected by chemiluminescence. The background levels of σNS and μNS in the BA and PI lanes represent nonspecific binding of these proteins to the beads.

in PBS. After blocking, cells were incubated for 1 h with primary antibodies, washed three times in PBS, and then incubated with secondary antibodies for 1 h. Immunostained cells were washed a final three times with PBS, incubated for 5 min in 300 nM 4′,6-diamidino-2-phenylindole, and mounted on slides with Prolong reagent (Molecular Probes). Immunostaining was alternatively performed using 1% bovine serum albumin in PBS as a blocking agent. Immunostained samples were examined using a Nikon TE-300 inverted microscope with fluorescence optics. Images were collected digitally as described elsewhere (28) and prepared for presentation using Photoshop and Illustrator software (Adobe Systems, San Jose, Calif.).

IP analysis. Infected or transfected cells were lysed by incubation for 30 min on ice in nondenaturing lysis (Raf) buffer (20 mM Tris [pH 8.0], 137 mM NaCl, 10% glycerol, 1% NP-40) (6) containing protease inhibitors (Roche Biochemicals, Indianapolis, Ind.). Because of nonspecific binding to protein A-conjugated beads by many of the proteins in this study, lysates were precleared for 1 h by incubation with 50 μl of a 50:50 slurry of protein A-Sepharose beads in Raf buffer, or with 50 μl of a 50:50 slurry of protein A-Sepharose beads in Raf buffer that were prebound to μNS preimmune antibody (9). After centrifugation at 13,000 × *g* to pellet protein A-conjugated beads and cell debris, lysates were transferred to new tubes. The protein concentration of each lysate was measured by Bradford assay (Bio-Rad) and normalized for relative protein concentration within each experiment. Immunoprecipitating antibodies that had been incubated for 2 h with protein A-conjugated magnetic beads (Dynal Biotech, Lake Success, N.Y.) and washed six times with Raf buffer were then added to the cell lysates, which were incubated, rotating, overnight at 4°C. Immunoprecipitated proteins were washed four times with Raf buffer and resuspended in sample buffer (125 mM Tris [pH 6.8], 10% sucrose, 1% [wt/vol] sodium dodecyl sulfate [SDS], 0.02% [vol/vol] β-mercaptoethanol, 0.01% bromophenol blue).

Immunoblot analysis. Immunoprecipitated proteins prepared as described above were boiled for 3 min and separated on SDS–10% polyacrylamide gel electrophoresis (PAGE) gels. Proteins were transferred to nitrocellulose by electroblotting in transfer buffer (25 mM Tris, 192 mM glycine, 20% methanol [pH 8.3]). Binding of primary antibodies was detected with HRP-conjugated secondary antibodies and Supersignal chemiluminescence reagent (Pierce). Supersignal-treated immunoblots were exposed to film to visualize bound HRP conjugates. Alternatively, binding of primary antibodies was detected with alkaline phosphatase-conjugated secondary antibodies and the colorimetric reagents *p*-nitroblue tetrazolium chloride and 5-bromo-4-chloro-3-indolylphosphate *p*-toluidine salt (Bio-Rad).

RNase ONE treatment. Proteins (with associated antibodies and protein A beads) immunoprecipitated as described above were split into two equal aliquots and resuspended in 10 μl of 10 mM Tris (pH 7.5). RNase ONE buffer (10 mM Tris-HCl [pH 7.5], 5 mM EDTA, 200 mM sodium acetate) was added to a 1× final concentration to both aliquots. Ten units of RNase ONE (Promega) was added to one aliquot, and both samples were incubated at 37°C for 30 min (23). After centrifugation at 13,000 × *g*, supernatants were removed from the pellets and sample buffer was added to both supernatants and pellets, which were then boiled and loaded on SDS-PAGE gels.

RESULTS

σNS and μNS colocalize in viral factories during reovirus

infection. Our laboratory has recently shown that nonstructural protein μNS localizes to, and is likely involved in the formation of, viral factories during reovirus infection (9). Other previous studies have indicated that the nonstructural protein σNS also localizes to these factories (5). To determine whether σNS and μNS colocalize in the factories, we examined the subcellular localization of σNS and μNS in T1L- and $T3D^N$-infected CV-1 cells by immunostaining with protein-specific antibodies at different times postinfection (p.i.). From the earliest time points that σNS and μNS were readily detectable (6 to 8 h p.i.), both proteins were found in a similar punctate pattern, with obvious regions of colocalization, throughout the cytoplasm (Fig. 1A, first and third rows). As infection proceeded, σNS and μNS continued to colocalize in the factories as they grew in size and moved to a perinuclear location (Fig. 1A, second and fourth rows). A difference in T1L (filamentous) and $T3D^N$ (globular) factory morphologies at 18 to 24 h p.i., which our laboratory has recently mapped to the M1 genome segment (28), was apparent in these experiments; however, this difference had no detectable effect on σNS and μNS colocalization, in that the two proteins colocalized in both types of factories (Fig. 1A, second and fourth rows). These findings suggest that a large portion of the σNS and μNS proteins in cells colocalize throughout infection.

σNS and μNS are coimmunoprecipitated from infected cells. The colocalization of σNS and μNS in viral factories suggests they may interact either directly or indirectly in infected cells. In addition, previous studies have shown that σNS and μNS, as well as outer-capsid protein σ3, can be coimmunoprecipitated from infected-cell lysates in complexes that also contain viral RNA (2). To extend our investigation of σNS-μNS associations, we examined the capacity of antibodies specific for σNS (or μNS) to coimmunoprecipitate μNS (or σNS) from infected cells. At 18 h p.i., CV-1 cells infected with either T1L or $T3D^N$ were lysed under nondenaturing conditions, followed by IP and immunoblotting with protein-specific antibodies. Following IP with μNS-specific antiserum and immunoblotting with σNS-specific antiserum, an ~40,000-M_r σNS band was recognized in both T1L- and $T3D^N$-infected cells in amounts that were increased over that in the control (Fig. 1B, left). Following IP with σNS-specific MAb and immunoblotting with μNS antiserum (8), an ~80,000-M_r μNS band was recognized in both T1L- and $T3D^N$-infected cells in amounts that were increased over that in the control (Fig. 1B, right). These data strongly suggest that σNS and μNS associate during infection but do not indicate if this is a direct interaction or if other components (such as RNA; see below) are needed to bridge these proteins.

σNS does not form inclusions when expressed alone in transfected cells. Previous reports have suggested that σNS nucleates viral factories (5). To determine if σNS forms factory-like inclusions when expressed in the absence of other viral proteins, we transfected CV-1 cells with pCI-S3(T1L) or pCI-S3(T3D). At 18 h posttransfection (p.t.), σNS was visualized by immunostaining with σNS MAb. σNS expressed from either the T1L S3 gene (Fig. 2A, top left) or the T3D S3 gene (http://micro.med.harvard.edu/nibert/suppl/miller03a/Fig.1.html) exhibited a diffuse distribution throughout the cytoplasm, with occasional cells also showing punctate staining in the nucleus. While these results do not rule out the possibility that σNS participates in forming the viral factories during infection, the diffuse cytoplasmic pattern of σNS staining seen here is inconsistent with σNS nucleating the factories independently of other viral components.

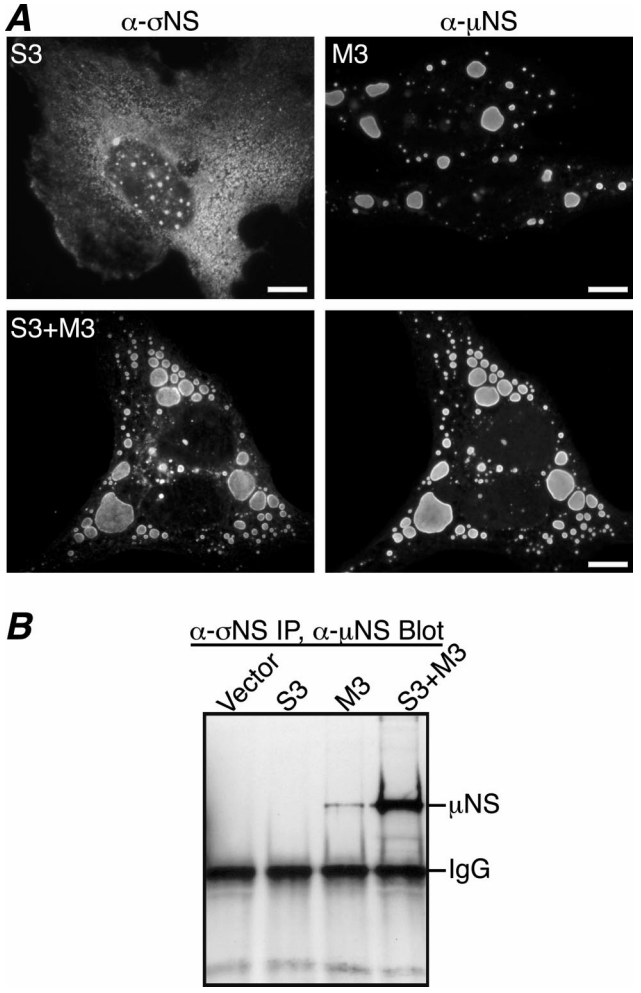

FIG. 2. Colocalization and co-IP of σNS and μNS in transfected CV-1 cells. (A) IF microscopy of CV-1 cells at 18 h p.t. with pCI-S3 (top left), pCI-M3 (top right), or both pCI-S3 and pCI-M3 (bottom row). σNS was visualized by immunostaining with σNS-specific mouse MAb 3E10 (5) followed by Alexa 488-conjugated anti-mouse IgG (left column). μNS was detected by immunostaining with Texas Red-conjugated μNS-specific polyclonal antibodies (9) (right column). Scale bars, 10 μm. (B) CV-1 cells transfected with pCI-neo (Vector), pCI-S3, pCI-M3, or both pCI-S3 and pCI-M3 were lysed in nondenaturing buffer and immunoprecipitated (IP) using σNS MAb. Immunoprecipitated proteins were separated by SDS-PAGE, transferred to nitrocellulose, and immunoblotted using μNS-specific rabbit polyclonal antiserum (8) followed by HRP-conjugated anti-rabbit IgG. Bound HRP conjugates were detected by chemiluminescence.

σNS is recruited to μNS inclusions when coexpressed in transfected cells. When expressed without other reovirus proteins in transfected cells, μNS forms smooth-edged, phase-dense globular inclusions that appear morphologically similar to viral factories (9) (Fig. 2A, top right). This finding, combined with our observation that σNS and μNS colocalize in the factories throughout infection, led us to hypothesize that σNS may be recruited to μNS inclusions when they are coexpressed.

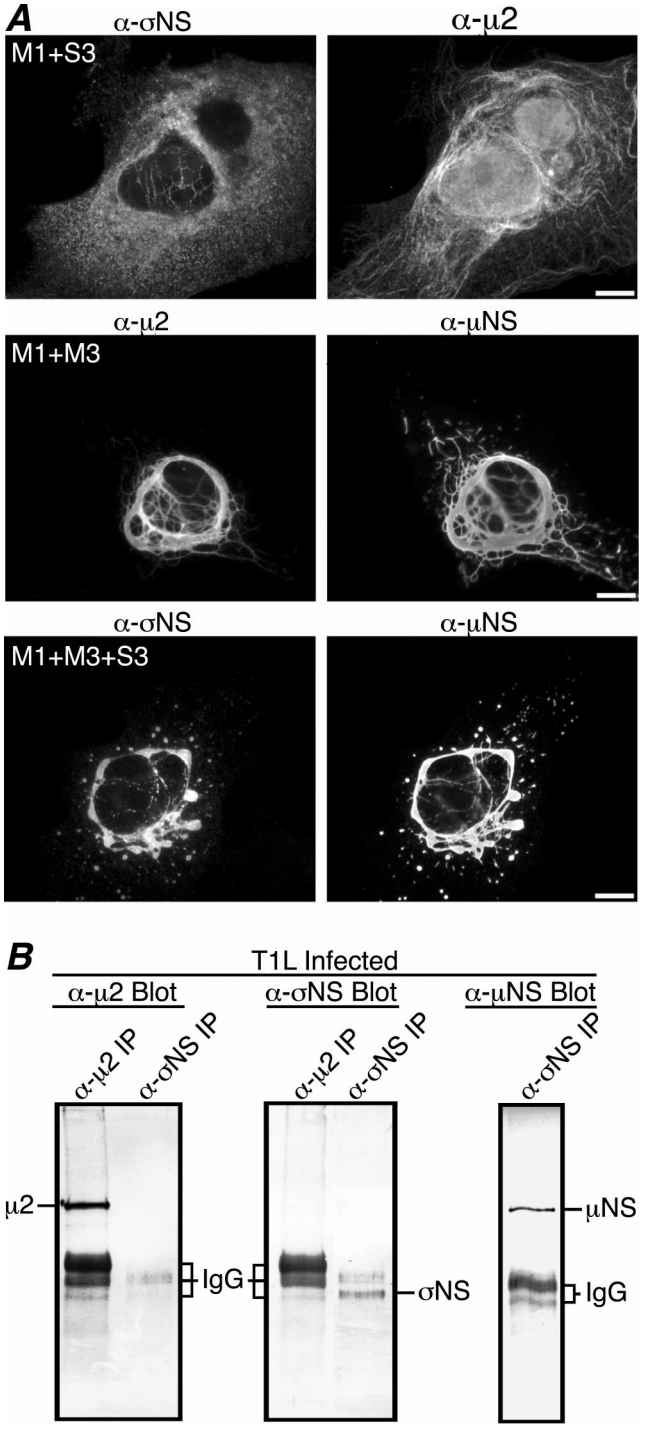

FIG. 3. μNS recruits σNS to filamentous inclusion-like structures when coexpressed with T1L μ2. (A) IF microscopy of CV-1 cells transfected with both pCI-S3 and pCI-M1(T1L) (top row), both pCI-M3 and pCI-M1(T1L) (middle row), or pCI-S3, pCI-M3, and pCI-M1(T1L) (bottom row). σNS was immunostained with σNS-specific mouse MAb 3E10 (5) followed by Alexa 488-conjugated anti-mouse IgG (top left and bottom left). μNS was immunostained with Texas Red-conjugated μNS-specific polyclonal antibodies (9) (middle right and bottom right). μ2 was immunostained with μ2-specific rabbit polyclonal antiserum (9) followed by Alexa 594-conjugated anti-rabbit IgG (middle left and top right). Scale bars, 10 μm. (B) μ2 and σNS do not coimmunoprecipitate. At 18 h p.i., T1L-infected CV-1 cells were lysed in nondenaturing buffer and immunoprecipitated (IP) using μ2 antiserum or σNS MAb. Immunoprecipitated proteins were separated by SDS-PAGE, transferred to nitrocellulose, and immunoblotted using μ2-specific (9) (left), σNS-specific (16) (middle), or μNS-specific (8) (right) rabbit polyclonal antiserum followed by alkaline phosphatase-conjugated anti-rabbit IgG. Bound alkaline phosphatase conjugates were detected by colorimetric staining.

To determine if expression of μNS alters σNS distribution, we cotransfected CV-1 cells with pCI-S3(T1L) and pCI-M3(T1L) and examined the localization of σNS and μNS by immunostaining with protein-specific antibodies at 18 h p.t. In this case, σNS staining was found primarily in discrete globular inclusions that colocalized with μNS in the cytoplasm (Fig. 2A, bottom row). To confirm the σNS-μNS association in cotransfected CV-1 cells, we tested whether the two proteins could be coimmunoprecipitated. At 18 h p.t., cells were lysed in nondenaturing buffer and IP was performed using σNS MAb. Following SDS-PAGE and transfer to nitrocellulose, proteins were visualized by immunoblotting with μNS antiserum. Consistent with immunostaining results, σNS MAb coimmunoprecipitated higher levels of μNS in the presence of σNS than in its absence (Fig. 2B). These results provide further evidence that σNS and μNS associate in cells and also indicate that this association results in recruitment of σNS to μNS inclusions when they are coexpressed in the absence of other viral proteins.

σNS and μ2 association in transfected cells. Our laboratory has recently identified the μ2 protein encoded by the reovirus M1 genome segment as a strain-specific microtubule-binding protein (28; J. Kim, J. S. L. Parker, and M. L. Nibert, submitted for publication). A difference in morphology of viral factories has also been mapped to the M1 segment, with M1(T1L)-containing viruses forming filamentous factories and M1($T3D^N$)-containing viruses forming globular factories (28). During T1L infection, σNS localizes to the filamentous factories (Fig. 1A, second row), which suggests that σNS might associate with μ2 as well as μNS. To determine if σNS colocalizes with μ2 in cells, we cotransfected CV-1 cells with pCI-S3 and pCI-M1(T1L) and examined the localization of both encoded proteins by immunostaining with protein-specific antibodies. When σNS was coexpressed with μ2(T1L), the μ2 protein was localized to thin filaments previously shown to be microtubules (28) (Fig. 3A, top right), while σNS retained a mostly diffuse staining pattern throughout the cytoplasm (Fig. 3A, top left). Although these results suggest that σNS does not colocalize with μ2, we sometimes observed faint filamentous staining of σNS in these experiments (Fig. 3A, top left) and were therefore prompted to examine further for an association with μ2 by determining whether σNS and μ2 could be coimmunoprecipitated. CV-1 cells were infected with T1L, and at 18 h p.i. nondenaturing IP using either μ2 antiserum or σNS MAb was performed on the cell lysates. Immunoprecipitated proteins were separated by SDS-PAGE, transferred to nitrocellulose, and immunoblotted using protein-specific antibodies. μ2 was precipitated by μ2 antiserum, but not by σNS MAb (Fig. 3B, left). Reciprocally, σNS was precipitated by σNS MAb, but not by μ2 antiserum (Fig. 3B, middle). As a control in this experiment, μNS was found to be coimmunoprecipitated by σNS MAb (Fig. 3B, right), as already noted above

(Fig. 1B). These results indicate that σNS and μ2(T1L) do not strongly associate. Similar results were obtained using lysates from transfected CV-1 cells expressing the σNS and μ2(T1L) proteins (data not shown). We also performed immunostaining to examine the localization of σNS when coexpressed with μ2(T3D) and did not detect any colocalization between these proteins (http://micro.med.harvard.edu/nibert/suppl/miller03a/Fig. 2.html). We conclude that σNS and μ2(T1L), when coexpressed in the absence of other viral proteins, might be weakly associated in cells but do not remain associated in cell lysates. Because μ2(T1L), but not μ2(T3D), induces microtubule bundling when expressed in cells (28), the faint filamentous pattern we observed when σNS was coexpressed with μ2(T1L) might reflect σNS association with bundled microtubules.

σNS is localized to filamentous inclusions when coexpressed with μNS and T1L μ2. Our laboratory has previously shown that when the M3 gene is cotransfected with M1(T1L), an association between μNS and μ2(T1L) results in recruitment of μNS and μ2(T1L) to thick filamentous structures that are colinear with microtubules (9) (Fig. 3A, middle row). This association of μNS with μ2, together with our new evidence that σNS strongly associates with μNS but not μ2 in transfected and infected cells, led us to hypothesize that μNS may recruit σNS to the μ2-bound microtubules. To test that possibility, we cotransfected pCI-S3, pCI-M3, and pCI-M1(T1L) into CV-1 cells and examined the localization of μNS and σNS by immunostaining with protein-specific antibodies. When σNS was coexpressed with both μNS and μ2, it was strikingly localized to filamentous structures, colocalizing with both μNS (Fig. 3A, bottom row) and μ2 (data not shown). This result confirms an association between σNS and μNS and further suggests that this association is important for recruiting σNS to filamentous factories during T1L infection.

μNS residues 1 to 40 are necessary for σNS localization to μNS inclusions. During reovirus infection, a second protein related to μNS, μNSC, is detected (24). μNS and μNSC share the same open reading frame, but μNSC is thought to lack the 40 N-terminal residues from μNS (38). It is not known if μNSC expression is required or plays some role(s) independent of μNS during infection. Our recent studies have shown that μNS(41-721), a recombinant form of μNS lacking residues 1 to 40, forms globular inclusions similar to those of μNS when expressed in the absence of other viral proteins (9). However, whereas μNS colocalizes with μ2 following coexpression, μNS(41-721) does not (9). These results prompted us to examine the localization of σNS in the presence of μNS(41-721) after cotransfecting CV-1 cells with pCI-S3 and pCI-M3(41-721) and immunostaining with protein-specific antibodies at 18 h p.t. As previously reported, the μNS(41-721) protein formed smooth-edged globular inclusions similar to those seen when μNS is expressed (Fig. 4A, right). The coexpressed σNS protein, in contrast, was found diffusely distributed throughout the cytoplasm and did not colocalize with the μNS(41-721) inclusions (Fig. 4A), suggesting that the N-terminal 40 residues of μNS are required for recruiting σNS. To examine further the lack of association between σNS and μNS(41-721), we cotransfected pCI-S3 and pCI-M3(41-721) into CV-1 cells and performed IP with either μNS antiserum or σNS MAb at 18 h p.t. Immunoprecipitated proteins were separated by SDS-PAGE, transferred to nitrocellulose, and immunoblotted with

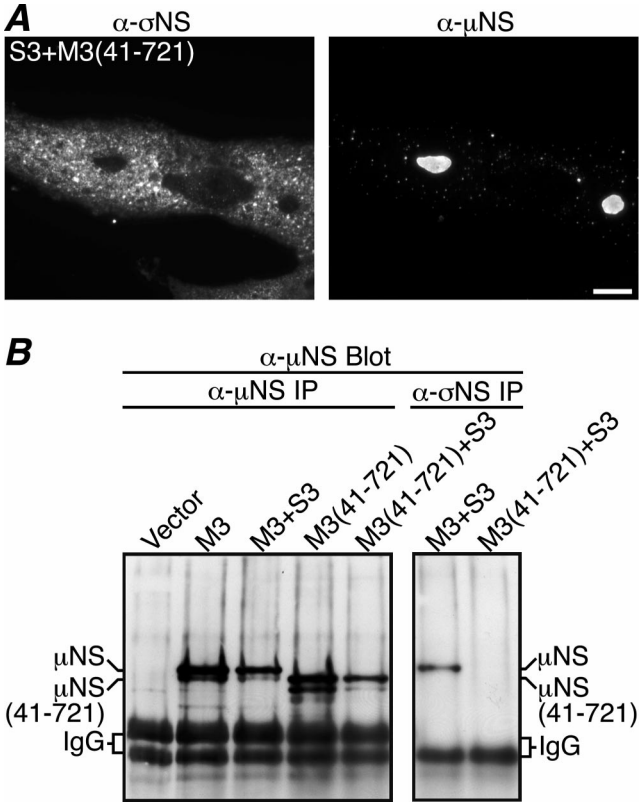

FIG. 4. μNS residues 1 to 40 are necessary for association with σNS. (A) IF microscopy of CV-1 cells transfected with both pCI-S3 and pCI-M3(41-721). At 18 h p.t., σNS and μNS(41-721) were, respectively, immunostained with σNS-specific mouse MAb 3E10 (5) followed by Alexa 488-conjugated anti-mouse IgG (left column) and Texas Red-conjugated μNS-specific polyclonal antibodies (9) (right column). Scale bar, 10 μm. (B) μNS(41-721) does not coimmunoprecipitate with σNS. At 18 h p.t. with pCI-neo (Vector), pCI-M3, both pCI-M3 and pCI-S3, pCI-M3(41-721), or both pCI-M3(41-721) and pCI-S3, CV-1 cells were lysed in nondenaturing buffer and immunoprecipitated (IP) using μNS-specific rabbit polyclonal antiserum (8) (left). In parallel, CV-1 cells transfected with both pCI-M3 and pCI-S3 or both pCI-M3(41-721) and pCI-S3 were lysed in nondenaturing buffer and immunoprecipitated with σNS MAb (right). Immunoprecipitated proteins were separated by SDS-PAGE, transferred to nitrocellulose, and immunoblotted using μNS antiserum followed by HRP-conjugated anti-rabbit IgG. Bound HRP conjugates were detected by chemiluminescence.

μNS antiserum. Consistent with the immunostaining results, μNS, but no detectable μNS(41-721), coimmunoprecipitated with σNS (Fig. 4B, right), even though similar amounts of μNS and μNS(41-721) were expressed (Fig. 4B, left). Several faster-mobility bands in both the μNS and the μNS(41-721) lanes likely resulted from protein degradation and did not coimmunoprecipitate with σNS (Fig. 4B). These results indicate that the N-terminal 40 residues of μNS, previously shown to associate with μ2 (9), are also necessary for association with σNS.

Associations with σNS and μ2 require different regions of the μNS N terminus. In an attempt to define more precisely the region of μNS required for its associations with σNS and μ2, we created a plasmid to express μNS lacking the first 13 residues from its N terminus [pCI-M3(14-721)] and examined the localization of σNS and μ2 when coexpressed with this

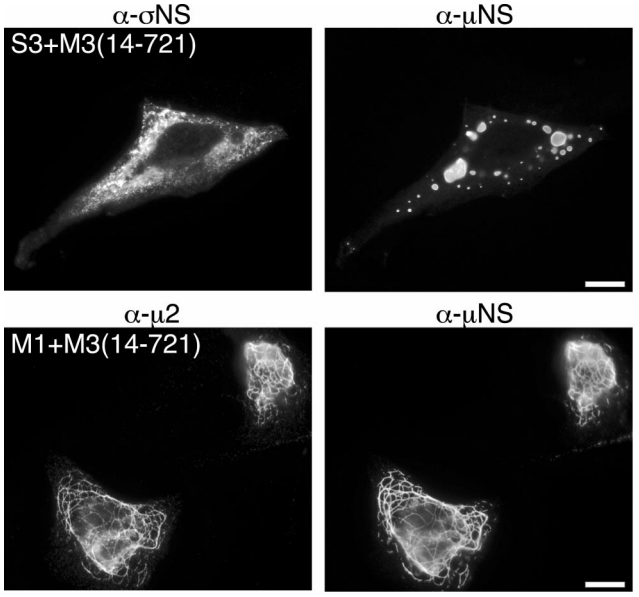

FIG. 5. Association of σNS and μ2 requires different regions of the μNS N terminus. IF microscopy of CV-1 cells at 18 h p.t. with both pCI-M3(14-721) and pCI-S3 (top row) or both pCI-M3(14-721) and pCI-M1(T1L) (bottom row) is shown. σNS was immunostained with σNS-specific mouse MAb 3E10 (5) followed by Alexa 488-conjugated anti-mouse IgG (top left). μ2 was immunostained with μ2-specific rabbit polyclonal antiserum (9) followed by Alexa 488-conjugated anti-rabbit IgG (bottom left). μNS was immunostained with Texas Red-conjugated μNS-specific polyclonal antibodies (9) (right column). Scale bars, 10 μm.

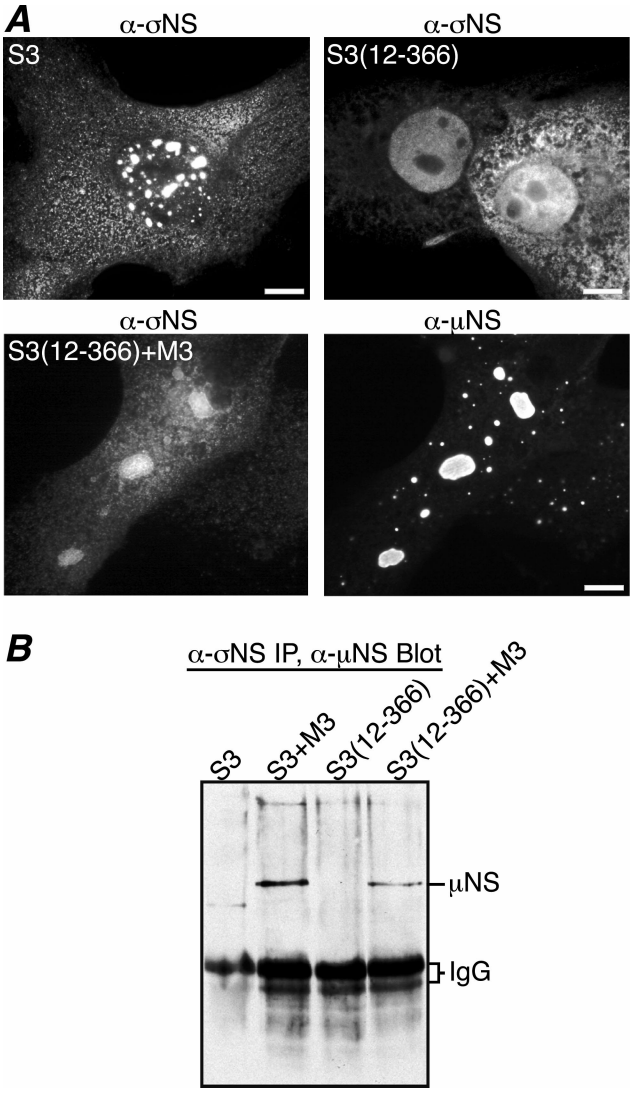

FIG. 6. σNS residues 1 to 11 are needed for maximal association with μNS. (A) IF microscopy of CV-1 cells at 18 h p.t. with pCI-S3 (top left), pCI-S3(12-366) (top right), or both pCI-S3(12-366) and pCI-M3 (bottom). σNS and σNS(12-366) were immunostained with σNS-specific mouse MAb 3E10 (5) followed by Alexa 488-conjugated anti-mouse IgG (top left and right and bottom left). μNS was immunostained with Texas Red-conjugated μNS-specific polyclonal antibodies (9) (bottom right). Scale bars, 10 μm. (B) Co-IP of μNS with σNS or σNS(12-366). At 18 h p.t. with pCI-S3, both pCI-S3 and pCI-M3, pCI-S3(12-366), or both pCI-S3(12-366) and pCI-M3, CV-1 cells were lysed in nondenaturing buffer and immunoprecipitated (IP) with σNS MAb. Immunoprecipitated proteins were separated by SDS-PAGE, transferred to nitrocellulose, and immunoblotted using μNS-specific rabbit polyclonal antiserum (8) followed by HRP-conjugated anti-rabbit IgG. Bound HRP conjugates were detected by chemiluminescence.

μNS truncation mutant. CV-1 cells were cotransfected with pCI-M3(14-721) and either pCI-S3 or pCI-M1(T1L) and then immunostained with protein-specific antibodies at 18 h p.t. When coexpressed with μNS(14-721), the σNS protein did not colocalize with the globular inclusions formed by μNS(14-721) and was instead found diffusely distributed throughout the cytoplasm (Fig. 5, top row). From these results we conclude that μNS residues 1 to 13 are required for σNS recruitment to μNS globular inclusions. When coexpressed with μ2, however, μNS(14-721), like μNS, was localized to μ2-positive filamentous structures, indicating that μNS residues 1 to 13 are not required for association with μ2 (Fig. 5, bottom row). These experiments suggest that separate regions within the μNS N terminus are necessary for the associations with σNS (μNS residues 1 to 13) and μ2 (μNS residues 14 to 41).

Deletion of σNS residues 1 to 11 reduces σNS association with μNS. Previous studies have shown that σNS is an ssRNA-binding protein (17, 18, 22), which when isolated from infected-cell lysates is found in large (40- to 60S) nucleoprotein complexes that are partially disassembled when treated with RNase A (18, 22). More recently it has been shown that recombinant σNS binds ssRNA and forms similar 40- to 60S nucleoprotein complexes and that a σNS mutant missing residues 1 to 11 is negative for these activities (16). To determine if the RNA-binding activity of σNS is required for its association with μNS, we created a mutant that lacks σNS residues 1 to 11 [pCI-S3(12-366)] and examined its subcellular localization by immunostaining. CV-1 cells were transfected with pCI-S3(12-366) in the presence or absence of pCI-M3 and were immunostained with protein-specific antibodies at 18 h p.t. The distribution of σNS(12-366) was similar to that previously seen for σNS, in that it was localized diffusely throughout the cytoplasm (Fig. 6A, top row). However, σNS(12-366) was also localized diffusely throughout the nucleus, whereas σNS was seen only in punctate dots within the nucleus (Fig. 6A, top row). The latter finding suggests that the nucleic acid-binding

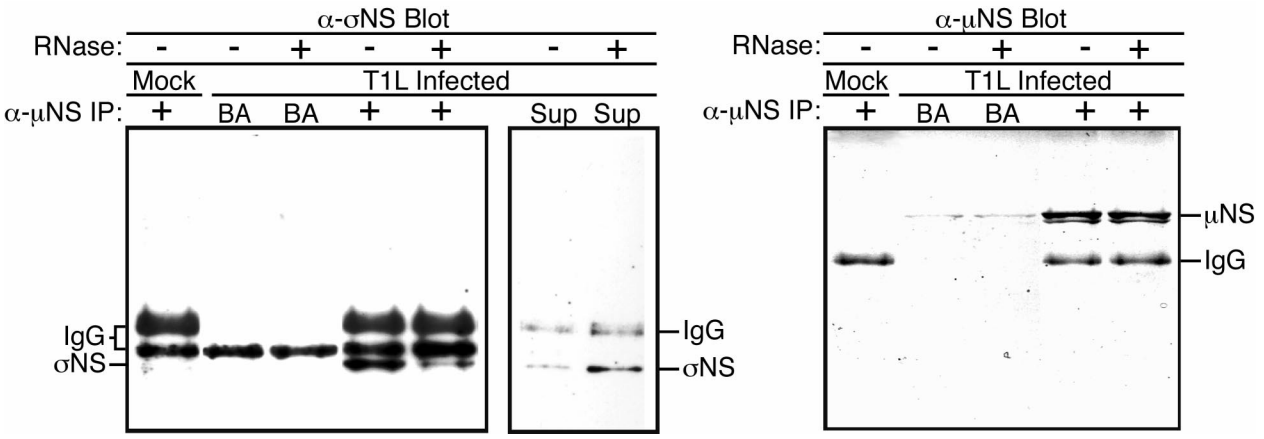

FIG. 7. σNS is complexed with both RNA and μNS in infected cells. (A) Mock- or T1L-infected CV-1 cells were lysed in nondenaturing buffer at 18 h p.i. and immunoprecipitated (IP) using μNS-specific rabbit polyclonal antiserum (8). IP with beads alone (BA) was used as a nonspecific-binding control. The immunoprecipitated proteins were split into two samples that were either treated or not treated with 10 U of RNase ONE (Promega). The samples were then resubjected to centrifugation, and the pellets (left and right) and supernatants (Sup) (middle) were subjected to SDS-PAGE. Proteins were transferred to nitrocellulose and immunoblotted using σNS-specific rabbit polyclonal antiserum (16) followed by HRP-conjugated anti-rabbit IgG (left and middle) or using μNS antiserum followed by HRP-conjugated anti-rabbit IgG (right). Bound HRP conjugates were detected by chemiluminescence.

activity of σNS may affect its distribution within the nucleus. When coexpressed with μNS, σNS(12-366) was again seen diffusely distributed throughout the nucleus and cytoplasm and, unlike σNS, only weakly localized to μNS inclusions (Fig. 6A, bottom row). This diffuse pattern with weak localization to μNS inclusions was seen even when 20-fold-more pCI-M3 than pCI-S3(12-366) was transfected into cells (data not shown). To confirm that σNS(12-366) has a diminished capacity to associate with μNS, we performed nondenaturing IP using the σNS MAb on lysates from CV-1 cells cotransfected with pCI-M3 and either pCI-S3 or pCI-S3(12-366). Following SDS-PAGE, proteins were transferred to nitrocellulose and immunoblotted using the μNS antiserum. Similar to the immunostaining results, σNS(12-366) association with μNS was diminished relative to that of σNS (Fig. 6B). While it has not been completely ruled out, it is unlikely that the σNS MAb shows diminished binding to σNS(12-366), since it appeared to bind well in immunostaining experiments (Fig. 6A, top right and bottom left). We also expressed carboxyl-terminally truncated forms of σNS to which this MAb only poorly reacts, suggesting it binds to a carboxyl-proximal epitope in σNS (data not shown). We conclude that σNS residues 1 to 11, previously shown to be required for RNA binding and nucleoprotein-complex formation (16), are also needed for optimal localization of σNS to μNS inclusions in transfected cells. We further hypothesized that RNA may contribute to the σNS-μNS association.

σNS is complexed with both RNA and μNS in infected cells. The preceding findings with σNS(12-366), along with previous evidence that σNS and μNS can be coimmunoprecipitated from infected cells in complexes that also contain viral ssRNA (2), prompted us to examine the role of RNA in the association of σNS and μNS observed in our experiments. We used μNS antiserum to coimmunoprecipitate σNS and μNS from T1L-infected CV-1 lysates. The immunoprecipitated proteins were then either left untreated or treated with RNase ONE (23) to determine if RNA digestion affected the σNS-μNS association. Following SDS-PAGE, proteins were transferred to nitrocellulose and probed with protein-specific antibodies. The amounts of σNS in the RNase ONE-treated immunoprecipitates were reduced compared to those in the untreated precipitates (Fig. 7, left). Moreover, supernatants from the RNase ONE-treated samples contained σNS at levels above those in the untreated supernatants (Fig. 7, middle). Similar amounts of μNS were confirmed to be present in the treated and untreated immunoprecipitates (Fig. 7, right). The results of these experiments suggest that a large portion of σNS in the μNS immunoprecipitates from infected cells is tethered through RNA, not μNS. The smaller portion of σNS that was not released from μNS immunoprecipitates by RNase ONE treatment, however, suggests that some σNS in infected cells might associate with μNS through an RNA-independent mechanism. Alternatively, the σNS and μNS that remain associated after RNase ONE treatment might be bridged by RNA protected from digestion. In either case, these data support a hypothesis in which σNS bound to RNA in the form of the previously reported large σNS-RNA complexes (16, 18, 22) localizes to viral factories through either protein-RNA or protein-protein interactions involving μNS.

σNS is complexed with both RNA and μNS in transfected cells. The preceding experiments indicate that a large portion of the σNS associated with μNS in infected cells is complexed with RNA. To determine if the σNS that associates with μNS in the absence of infection is also complexed with RNA, we cotransfected cells with pCI-S3 and pCI-M3 and performed nondenaturing IP using the μNS antiserum on the transfected-cell lysates. Immunoprecipitates were either left untreated or treated with RNase ONE, then separated by SDS-PAGE, transferred to nitrocellulose, and immunoblotted with either the μNS antiserum or the σNS MAb. σNS was found in large amounts in the untreated immunoprecipitates but in reduced amounts in the precipitates treated with RNase ONE (Fig. 8, left). Moreover, supernatants from the RNase ONE-treated samples contained σNS at levels clearly above those in the untreated samples (Fig. 8, middle). Similar amounts of μNS

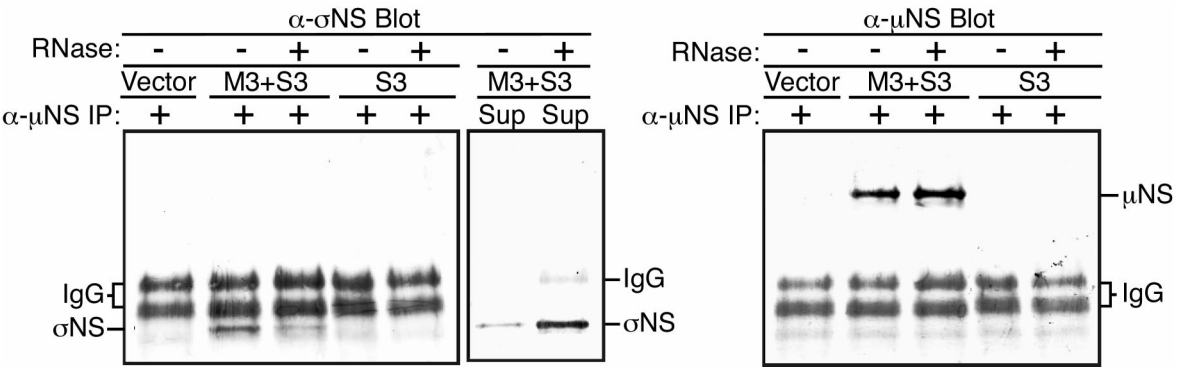

FIG. 8. σNS is complexed with both RNA and μNS in transfected cells. CV-1 cells transfected with pCI-neo (Vector), pCI-S3, or both pCI-M3 and pCI-S3 were lysed in nondenaturing buffer at 18 h p.t. and immunoprecipitated (IP) using μNS-specific rabbit polyclonal antiserum (8). The immunoprecipitated proteins were split into two samples, which were either treated or not treated with 10 U of RNase ONE (Promega). The samples were then resubjected to centrifugation, and the pellets (left and right) and supernatants (Sup) (middle) were subjected to SDS-PAGE. Proteins were transferred to nitrocellulose and immunoblotted using σNS-specific mouse MAb 3E10 (5) followed by HRP-conjugated anti-mouse IgG (left and middle) or μNS antiserum followed by HRP-conjugated anti-rabbit IgG (right). Bound HRP conjugates were detected by chemiluminescence.

were confirmed to be present in the treated and untreated immunoprecipitates (Fig. 8, right). These results show that a large portion of the σNS coimmunoprecipitated with μNS from transfected cells is tethered through RNA, and not μNS, in the absence of either native viral RNA or other viral proteins. These data suggest that the RNA complexed by σNS when associating with μNS may not need to be viral in nature, although it is possible that the complexed RNA in these experiments was generated from the σNS and μNS expression clones. The RNA component of these complexes is currently under investigation.

DISCUSSION

Role of σNS in reovirus factory formation. σNS has been previously reported to nucleate viral factories, based on evidence that it is localized to factories throughout infection and that mutant *ts*E320, which has a temperature-sensitive σNS protein, does not form detectable factories at restrictive temperatures (5). Further examination in this study showed that when expressed in the absence of other viral proteins, σNS was distributed diffusely throughout the cytoplasm (Fig. 2A). In contrast, the μNS protein forms phase-dense inclusions with a morphology very similar to that of the globular viral factories that form in some infected cells (9) (Fig. 2A). It was only when σNS was coexpressed with μNS that σNS localized to these inclusions (Fig. 2A). Taken together, these results support the conclusion that σNS localizes to viral factories by associating with μNS and is not itself the nucleating factor.

σNS may nonetheless play a regulatory role in factory formation (25a). While σNS coexpression with μNS did not alter the shape or localization of μNS inclusions, it often resulted in many smaller inclusions that were juxtaposed in the cytoplasm (Fig. 2A). A possible explanation is that association of σNS with μNS interferes with μNS-μNS interactions and consequently prevents smaller μNS inclusions from merging to form larger ones. Whether this has any implications for the roles of σNS (and μNS) in infection remains to be determined. σNS may also play a role in recruiting RNA to the factories (see below).

Previous results suggesting a defect in factory formation by the *ts*E320 mutant can probably be explained by this strain's defect in protein production (5). Our laboratory has previously reported that the size of the μNS inclusions is dependent on the amount of protein expressed (9); thus, a defect in protein production would likely lead to reduced formation of larger factories. When we introduced the *ts*E320 mutation into the σNS expression plasmid [pCI-S3(M260T)], we found that in most transfected cells it formed large aggregates at restrictive temperature, typical of misfolded proteins (data not shown). Although this mutant σNS did not localize to μNS inclusions when coexpressed with μNS at restrictive temperature (data not shown), we think this was likely because the protein was misfolded and nonfunctional in many respects and not because of a specific defect in μNS association. At permissive temperature, localization of σNS(*ts*E320) in the absence or presence of μNS was similar to that of wild-type σNS (data not shown). It remains to be determined which specific functions of σNS are responsible for the defects in protein and viral dsRNA production exhibited by the *ts*E320 mutant (10, 14).

σNS association with the N terminus of μNS. A previous study has shown that μNS residues 1 to 40 or 41 are both necessary and sufficient for association with μ2 (28). We showed in this study that the N-terminal 40 amino acids of μNS were also necessary for association with σNS (Fig. 4). Additionally, we dissected this region of μNS into two smaller regions by showing that deletion of μNS residues 1 to 13 resulted in loss of σNS association with μNS but had no effect on μ2 association with μNS (Fig. 5). These findings are especially interesting because a second form of μNS, called μNSC, thought to lack 40 residues from the N terminus of μNS is expressed during infection (24, 38). It is not known if μNSC performs the same functions as μNS or has some distinct role(s). The findings that μNS can associate strongly with both σNS and the viral microtubule-associated protein μ2 (9), whereas μNS(41-721) can associate with neither, support the

hypothesis that μNS and μNSC are involved in some different processes. Like μNS, μNS(41-721) forms factory-like inclusions in transfected cells (9) and also binds viral core particles in vitro (T. J. Broering, P. L. Joyce, and M. L. Nibert, unpublished data). Based on these findings, we propose that the production of both μNS and μNSC might be needed as part of a regulatory mechanism to balance RNA assortment, minus-strand synthesis, and core assembly within viral factories. In particular, μNS, which can associate with both σNS and μ2, might promote RNA-related processes, whereas μNSC, which can associate with neither σNS nor μ2 but can still interact with one or more of the core surface proteins (Broering et al., unpublished), might promote capsid assembly-related processes.

Even though we defined two distinct regions of the μNS N terminus required for association with σNS and μ2, we have not yet determined if the same molecule of μNS can associate with both proteins simultaneously or if instead σNS and μ2 must associate with different molecules of μNS. μNS may act to recruit proteins to viral factories such that they can perform their roles in RNA assortment, minus-strand synthesis, and core assembly. In addition, μNS, by associating with several proteins at once, may act to bring these proteins (e.g., σNS and μ2) into close proximity and in particular orientations to perform specific functions within the factories. We have also not yet demonstrated that a region of the μNS N terminus is sufficient for association with σNS.

Complexes containing μNS, σNS, and RNA. σNS is an ssRNA-binding protein that is isolated from infected cells in large RNA-containing complexes (16, 18, 22). The N-terminal 11 residues of σNS have been previously shown to be required for both optimal ssRNA binding and formation of the large σNS-RNA complexes (16). We showed in this study that deletion of σNS residues 1 to 11 diminished, but did not eliminate, the capacity of σNS to associate with μNS (Fig. 6). These results suggest that RNA contributes to the σNS association with μNS. We further addressed the role of RNA by examining the effect of RNase treatment on σNS and μNS association in immunoprecipitated complexes from either infected (Fig. 7) or transfected (Fig. 8) cells. Those studies showed that while a large portion of σNS was released from μNS when treated with RNase ONE, a smaller portion of σNS remained associated with μNS even following this treatment. This finding suggests that some σNS might associate with μNS independently of RNA. In any case, much of the σNS associated with μNS is in the form of σNS-RNA complexes in both infected and transfected cells. Whether RNA binding alters the conformation of σNS to enhance μNS association remains unknown; however, the diminished levels of μNS association with σNS(12-366) might indicate that there is a higher-affinity or -avidity interaction between σNS and μNS when σNS is complexed with RNA.

μNS, σNS, and the structural protein σ3 were previously shown to be coimmunoprecipitated from infected cells in complexes that contain viral ssRNA (2). While there is strong evidence that σNS is an ssRNA-binding protein (17, 18, 22) and σ3 is a dsRNA-binding protein (22, 32), it is not known if μNS binds either ss- or dsRNA. Our results showed that σNS associated with μNS in viral factories as soon as either protein was detectable in infected cells (Fig. 1) and that, when μNS

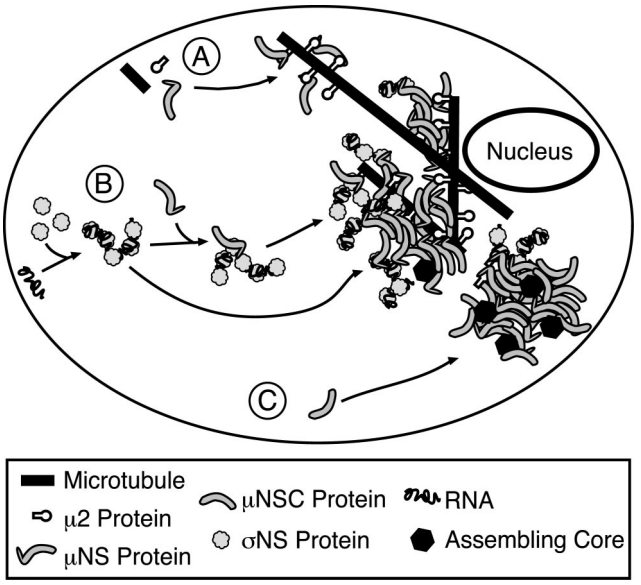

FIG. 9. Model of reovirus protein associations and factory assembly. (A) With most reovirus strains, μ2 associates with cellular microtubules and anchors viral factories to them through association with the μNS N terminus (9, 28). (B) σNS, complexed with RNA, is also recruited to viral factories by association with the N terminus of μNS (this study). σNS may associate with a μNS molecule before joining the factory (top path) or, alternatively, it might bind to μNS already within the factory (bottom path). (C) μNSC does not bind σNS (this study) or μ2 (9), but it does form globular inclusions (9) and does associate with core surface proteins (Broering et al., unpublished), suggesting it is involved in some distinct steps in the replication cycle.

immunoprecipitates were treated with RNase ONE, a large portion of σNS was released into the supernatant while only a smaller portion of σNS remained associated with μNS on the beads (Fig. 7). This raises the possibility that the RNA immunoprecipitated using a μNS-specific MAb in the previous studies (2) was not bound to μNS but was instead bound to the associated σNS. The RNA-binding properties of μNS are currently under investigation.

The nature of the RNA coimmunoprecipitated with σNS and μNS in our experiments remains unknown. σNS binds RNA in a sequence-independent manner in vitro (17, 30), and in the present studies it was bound to RNA in cells in the absence of infection (Fig. 8). It is possible that the bound RNA was derived from the σNS and μNS expression vectors, but this has not been tested. Previous evidence that ssRNA derived from each of the 10 genome segments can be coimmunoprecipitated with σNS, μNS, and σ3 from infected-cell lysates (2) has been used to suggest that these proteins cooperate in forming early replication complexes. Our results add to this hypothesis by suggesting that the complexes containing RNA, σNS, and μNS are localized to viral factories through either direct or indirect association of σNS with the N terminus of μNS. We did not examine the localization of σ3 in this study.

Overview: specific protein-protein associations in reovirus factories. Our recent and ongoing studies are identifying a series of specific protein-protein associations involved in forming, and recruiting proteins and RNA to, the viral factories in reovirus-infected cells (Fig. 9). To date, we have identified the

80-kDa nonstructural protein μNS as a key player in these associations. μ2 and σNS, the latter in the form of RNA-containing complexes, specifically associate with μNS through a mechanism requiring the μNS N terminus (28). Other evidence suggests that one or more of the surface proteins in viral cores (λ1, λ2, or σ2) associates with the more-carboxyl-terminal regions of μNS contained in μNSC (38) (Broering et al., unpublished). Our current hypothesis is that μNS and μNSC are further required during reovirus infection for specifically organizing the viral and cellular factors involved in RNA recruitment and assortment, minus-strand synthesis, and core assembly within the factories.

ACKNOWLEDGMENTS

We thank Michelle Becker, Terry Dermody, and coworkers for providing the σNS-specific MAb used in these studies. We also thank Jonghwa Kim for sharing his μ2 antiserum, Caroline Piggott for performing antibody titrations, Elaine Freimont and Jason Dinoso for laboratory maintenance and technical assistance, and other members of our laboratory for helpful discussions.

This work was supported by NIH grants RO1 AI47904 (to M.L.N.) and K08 AI52209 (to J.S.L.P) and a junior faculty research grant from the Giovanni Armenise—Harvard Foundation (to M.L.N.). C.L.M. and T.J.B. received additional, respective, support from NIH grant T32 AI07061 to the Combined Infectious Diseases Training Program at Harvard Medical School and NIH grant T32 AI07245 to the Viral Infectivity Training Program at Harvard Medical School.

REFERENCES

1. **Acs, G., H. Klett, M. Schonberg, J. Christman, D. H. Levin, and S. C. Silverstein.** 1971. Mechanism of reovirus double-stranded ribonucleic acid synthesis in vivo and in vitro. J. Virol. **8:**684–689.
2. **Antczak, J. B., and W. K. Joklik.** 1992. Reovirus genome segment assortment into progeny genomes studied by the use of monoclonal antibodies directed against reovirus proteins. Virology **187:**760–776.
3. **Banerjee, A. K., and A. J. Shatkin.** 1970. Transcription in vitro by reovirus-associated ribonucleic acid-dependent polymerase. J. Virol. **6:**1–11.
4. **Bartlett, N. M., S. C. Gillies, S. Bullivant, and A. R. Bellamy.** 1974. Electron microscopy study of reovirus reaction cores. J. Virol. **14:**315–326.
5. **Becker, M. M., M. I. Goral, P. R. Hazelton, G. S. Baer, S. E. Rodgers, E. G. Brown, K. M. Coombs, and T. S. Dermody.** 2001. Reovirus σNS protein is required for nucleation of viral assembly complexes and formation of viral inclusions. J. Virol. **75:**1459–1475.
6. **Bodendorf, U., C. Cziepluch, J. C. Jauniaux, J. Rommelaere, and N. Salome.** 1999. Nuclear export factor CRM1 interacts with nonstructural proteins NS2 from parvovirus minute virus of mice. J. Virol. **73:**7769–7779.
7. **Borsa, J., M. D. Sargent, P. A. Lievaart, and T. P. Copps.** 1981. Reovirus: evidence for a second step in the intracellular uncoating and transcriptase activation process. Virology **111:**191–200.
8. **Broering, T. J., A. M. McCutcheon, V. E. Centonze, and M. L. Nibert.** 2000. Reovirus nonstructural protein μNS binds to core particles but does not inhibit their transcription and capping activities. J. Virol. **74:**5516–5524.
9. **Broering, T. J., J. S. L. Parker, P. L. Joyce, J. Kim, and M. L. Nibert.** 2002. Mammalian reovirus nonstructural protein μNS forms large inclusions and colocalizes with reovirus microtubule-associated protein μ2 in transfected cells. J. Virol. **76:**8285–8297.
10. **Cross, R. K., and B. N. Fields.** 1972. Temperature-sensitive mutants of reovirus type 3: studies on the synthesis of viral RNA. Virology **50:**799–809.
11. **Dales, S.** 1963. Association between the spindle apparatus and reovirus. Proc. Natl. Acad. Sci. USA **50:**268–275.
12. **Dales, S., P. Gomatos, and K. C. Hsu.** 1965. The uptake and development of reovirus in strain L cells followed with labelled viral ribonucleic acid and ferritin-antibody conjugates. Virology **25:**193–211.
13. **Faust, M., K. E. Hastings, and S. Millward.** 1975. $m^7G^{5'}ppp^{5'}GmpCpUp$ at the 5′ terminus of reovirus messenger RNA. Nucleic Acids Res. **2:**1329–1343.
14. **Fields, B. N., and W. K. Joklik.** 1969. Isolation and preliminary genetic and biochemical characterization of temperature-sensitive mutants of reovirus. Virology **37:**335–342.
15. **Furuichi, Y., S. Muthukrishnan, J. Tomasz, and A. J. Shatkin.** 1976. Mechanism of formation of reovirus mRNA 5′-terminal blocked and methylated sequence, m^7GpppG^mpC. J. Biol. Chem. **251:**5043–5053.
16. **Gillian, A. L., and M. L. Nibert.** 1998. Amino terminus of reovirus nonstructural protein σNS is important for ssRNA binding and nucleoprotein complex formation. Virology **240:**1–11.
17. **Gillian, A. L., S. C. Schmechel, J. Livny, L. A. Schiff, and M. L. Nibert.** 2000. Reovirus nonstructural protein σNS binds in multiple copies to single-stranded RNA and shares properties with single-stranded DNA binding proteins. J. Virol. **74:**5939–5948.
18. **Gomatos, P. J., O. Prakash, and N. M. Stamatos.** 1981. Small reovirus particle composed solely of sigma NS with specificity for binding different nucleic acids. J. Virol. **39:**115–124.
19. **Gomatos, P. J., N. M. Stamatos, and N. H. Sarkar.** 1980. Small reovirus-specific particle with polycytidylate-dependent RNA polymerase activity. J. Virol. **36:**556–565.
20. **Harrison, S. J., D. L. Farsetta, J. Kim, S. Noble, T. J. Broering, and M. L. Nibert.** 1999. Mammalian reovirus L3 gene sequences and evidence for a distinct amino-terminal region of the λ1 protein. Virology **258:**54–64.
21. **Haut, D. D., and D. J. Pintel.** 1998. Intron definition is required for excision of the minute virus of mice small intron and definition of the upstream exon. J. Virol. **72:**1834–1843.
22. **Huismans, H., and W. K. Joklik.** 1976. Reovirus-coded polypeptides in infected cells: isolation of two native monomeric polypeptides with affinity for single-stranded and double-stranded RNA, respectively. Virology **70:**411–424.
23. **Khorchid, A., R. Halwani, M. A. Wainberg, and L. Kleiman.** 2002. Role of RNA in facilitating Gag/Gag-Pol interaction. J. Virol. **76:**4131–4137.
24. **Lee, P. W. K., E. C. Hayes, and W. K. Joklik.** 1981. Characterization of anti-reovirus immunoglobulins secreted by cloned hybridoma cell lines. Virology **108:**134–146.
25. **Mayor, H. D.** 1965. Studies on reovirus. 3. A labile, single-stranded ribonucleic acid associated with the late stages of infection. J. Natl. Cancer Inst. **35:**919–925.

25a. **Mbisa, J. L., M. M. Becker, S. Zou, T. S. Dermody, and E. G. Brown.** 2000. Reovirus μ2 protein determines strain-specific differences in the rate of viral inclusion formation in L929 cells. Virology **272:**16–26.

26. **Nibert, M. L.** 1998. Structure of mammalian orthoreovirus particles. Curr. Top. Microbiol. Immunol. **238:**1–30.
27. **Nibert, M. L., L. A. Schiff, and B. N. Fields.** 2001. Reoviruses and their replication, p. 1679–1728. *In* D. M. Knipe and P. M. Howley (ed.), Field's virology, 4th ed. Lippincott Williams & Wilkins, Philadelphia, Pa.
28. **Parker, J. S. L., T. J. Broering, J. Kim, D. E. Higgins, and M. L. Nibert.** 2002. Reovirus core protein μ2 determines the filamentous morphology of viral inclusion bodies by interacting with and stabilizing microtubules. J. Virol. **76:**4483–4496.
29. **Rhim, J. S., L. E. Jordan, and H. D. Mayor.** 1962. Cytochemical, fluorescent-antibody and electron microscopic studies on the growth of reovirus (ECHO 10) in tissue culture. Virology **17:**342–355.
30. **Richardson, M. A., and Y. Furuichi.** 1985. Synthesis in *Escherichia coli* of the reovirus nonstructural protein σ_{NS}. J. Virol. **56:**527–533.
31. **Sakuma, S., and Y. Watanabe.** 1971. Unilateral synthesis of reovirus double-stranded ribonucleic acid by a cell-free replicase system. J. Virol. **8:**190–196.
32. **Schiff, L. A., M. L. Nibert, M. S. Co, E. G. Brown, and B. N. Fields.** 1988. Distinct binding sites for zinc and double-stranded RNA in the reovirus outer capsid protein σ3. Mol. Cell. Biol. **8:**273–283.
33. **Silverstein, S. C., C. Astell, D. H. Levin, M. Schonberg, and G. Acs.** 1972. The mechanisms of reovirus uncoating and gene activation in vivo. Virology **47:**797–806.
34. **Silverstein, S. C., and S. Dales.** 1968. The penetration of reovirus RNA and initiation of its genetic function in L-strain fibroblasts. J. Cell Biol. **36:**197–230.
35. **Silverstein, S. C., and P. H. Schur.** 1970. Immunofluorescent localization of double-stranded RNA in reovirus-infected cells. Virology **41:**564–566.
36. **Skup, D., and S. Millward.** 1980. Reovirus-induced modification of cap-dependent translation in infected L cells. Proc. Natl. Acad. Sci. USA **77:**152–156.
37. **Stamatos, N. M., and P. J. Gomatos.** 1982. Binding to selected regions of reovirus mRNAs by a nonstructural reovirus protein. Proc. Natl. Acad. Sci. USA **79:**3457–3461.
38. **Wiener, J. R., J. A. Bartlett, and W. K. Joklik.** 1989. The sequences of reovirus serotype 3 genome segments M1 and M3 encoding the minor protein μ2 and the major nonstructural protein μNS, respectively. Virology **169:**293–304.
39. **Wiener, J. R., and W. K. Joklik.** 1987. Comparison of the reovirus serotype 1, 2, and 3 S3 genome segments encoding the nonstructural protein σNS. Virology **161:**332–339.
40. **Zweerink, H. J., Y. Ito, and T. Matsuhisa.** 1972. Synthesis of reovirus double-stranded RNA within virionlike particles. Virology **50:**349–358.
41. **Zweerink, H. J., and W. K. Joklik.** 1970. Studies on the intracellular synthesis of reovirus-specified proteins. Virology **41:**501–518.